

Self-Organized Formation of Hexagonal Pore Structures in Anodic Alumina

O. Jessensky, F. Müller, and U. Gösele

Max-Planck-Institut für Mikrostrukturphysik, D-06120 Halle, Germany

ABSTRACT

The morphology and formation conditions of ordered hexagonal pore arrays in anodic alumina are discussed. The ordered arrangement of pores is shown to form by a self-organized process starting from randomly distributed pore positions at the surface of the alumina. The influence of the pretreatment of the aluminum substrate and the anodizing conditions on the growth kinetics and the tendency to form hexagonal pore structures were investigated. Homogeneous etching conditions are required in order to obtain regular pore arrays. This observation corresponds to the finding that hexagonal pore arrays are related to a smooth etching front and a homogeneous depth of neighboring pores.

Porous anodic alumina is a widely studied material that is used for corrosion protection of aluminum surfaces or as dielectric material in microelectronics applications. For more than 40 years porous alumina has been the subject of investigations.¹ It exhibits a homogeneous morphology of parallel pores which grow perpendicular to the surface with a narrow distribution of diameters and interpore spacings, the size of which can easily be controlled between 10 and some 100 nm. Because of these properties, it has been applied as a template for the fabrication of nanometer-scale composites.²⁻⁴ Self-organization during pore growth that leads to a densely packed hexagonal pore structure has just recently been reported.⁵⁻⁸ The self-organized arrangement of neighboring pores in ordered hexagonal arrays can only be explained by a repulsive interaction between the pores during growth. Mechanical stress due to the volume expansion during aluminum oxidation has been proposed by the authors to be the origin of these repulsive forces.⁹ In the present work, we focus on the influence of anodization conditions and pretreatment of the starting aluminum on the process of pore growth and self-organized formation of ordered pore arrays.

Experimental

High purity (99.999%) aluminum foils from Goodfellow were mounted on a copper plate serving as the anode. A circular area of 1 cm diam was exposed to the acid in a thermally insulated electrochemical cell. While the anode temperature was kept constant at 1°C, the temperature of the electrolyte deviated from that value by less than 0.1 K. The low anodization temperature was chosen in order to achieve low pore growth rates. Low growth rates are most likely favorable for the process of self-organization. As in the work of Masuda and Fukuda,⁵ 0.3 M oxalic acid was used as the electrolyte. The anodization voltage was varied between 30 and 60 V. With pore growth rates of 1–2 $\mu\text{m}/\text{h}$ and etching times between 2 to 4 days, a layer thickness between 100 to 200 μm , and aspect ratios (ratios of pore diameter to depth) of more than 1000 were obtained.

Besides applying appropriate anodization parameters, the pretreatment of the aluminum foils turned out to be important for the formation of ordered pore arrays. In addition, the stirring of the electrolyte during anodization was a necessary condition for the formation of ordered pore arrays. After a discussion of the morphological features of the pore structures and their voltage-dependent growth kinetics, the influence of both the pre-anodizing treatment and the anodization conditions on the morphological features, especially for formation of ordered pore arrays, is analyzed in detail.

Morphology

After anodization, the remaining aluminum was removed in a saturated HgCl_2 solution. Afterward, the spherically shaped pore bottoms could be observed at the lower surface of the alumina. Figure 1 shows scanning electron microscopy (SEM) images of the top and the bottom view of the

alumina after dissolution of the aluminum. Although the pores start growing at the upper surface at almost random positions, nearly perfectly ordered densely packed hexagonal structures can be observed at the bottom of the layer. This ordered structure is accompanied by a smooth lower surface and a homogeneous depth of neighboring pores. The pore density in ordered pore arrays was found to be typically about 20% lower than at the upper surface of the alumina, indicating that part of the pores stop growing either shortly after their nucleation or during the self-organization process.

In order to examine the relationship between the degree of ordering and the smoothness of the etching front, the bottom surface of the alumina was studied with atomic force microscopy (AFM). Figure 2 shows an AFM image of an alumina layer which contained hexagonally ordered domains as well as areas with a lower degree of ordering. While in general a surface roughness of less than 30 nm is observed over the image area, the differences in height between

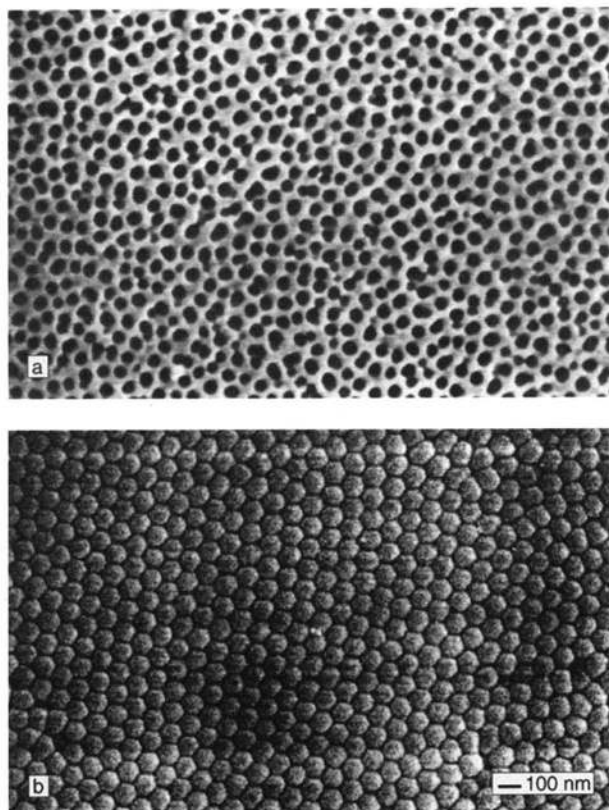
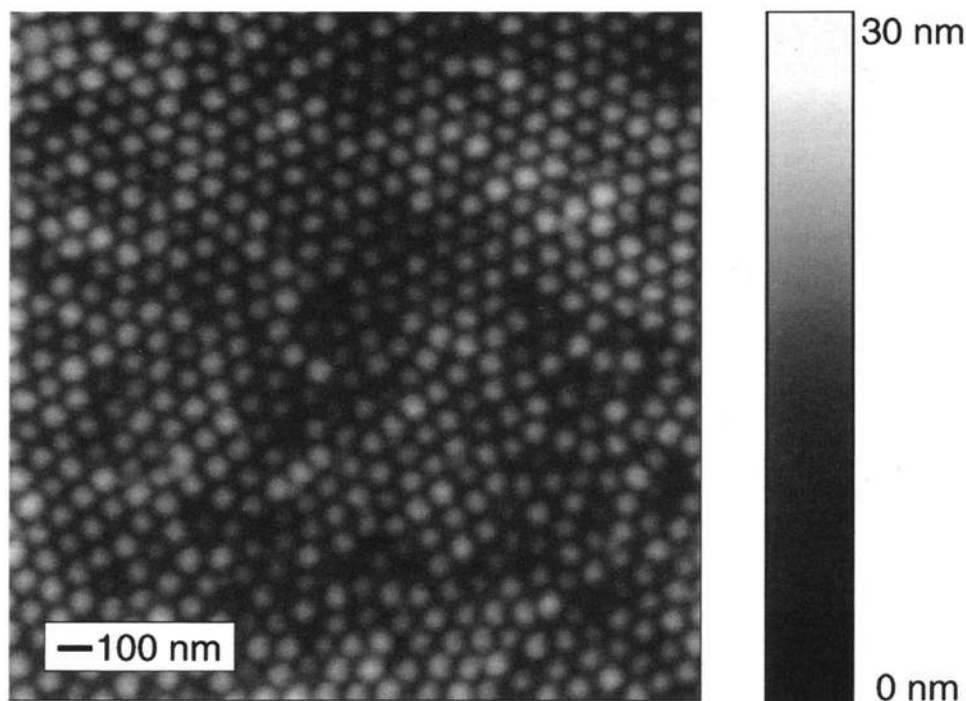


Fig. 1. SEM top view (upper image) and bottom view after dissolution of the remaining aluminum (lower image) of an anodic alumina layer [40 V, 0.3 M $(\text{COOH})_2$, 1°C].

Fig. 2. AFM image (bottom view) of an anodic alumina layer showing ordered and non-ordered areas [30 V, 0.3 M (COOH)₂, 1°C].



neighboring pores are lower in regions with a high degree of ordering compared to nonordered areas. We conclude that the hexagonal ordering of the pores within the plane of the etching front is correlated with a homogeneous pore depth within the ordered areas.

By chemical etching in 5 wt % aqueous phosphoric acid, opening of the pore bottoms as well as widening of the pores was achieved. In Fig. 3, a SEM bottom view of a porous alumina layer after dissolution of the pore bottoms is shown at a lower magnification. Perfect hexagonal pore arrays are observed within domains of micron size, which are separated from neighboring domains with a different orientation of the pore lattice by grain boundaries. Thus, a polycrystalline pore structure is observed. The structures with the highest degree of ordering were obtained at 40 V anodizing voltage, which corresponds to the anodization parameters given by Masuda and Fukuda.⁵

The degree of ordering was reproducible with this set of parameters. The lattice constant within the ordered domains was approximately proportional to the forming voltage, in accordance with the literature, where proportionality of both pore and cell wall diameters to the voltage has been established.^{9,10}

The bottom view of a nonordered alumina layer formed with 40 V in 0.3 M oxalic acid without stirring of the elec-

trolyte is shown in Fig. 4. The pores form a pseudo-hexagonal structure being surrounded by an average of six nearest neighbors, but an ordered hexagonal lattice cannot be observed. Because this structure deviates from the densely packed hexagonal lattice, the pore density is more than 20% lower than in ordered arrays produced with the same anodizing voltage and the pores shape is not circular anymore.

The difference in the morphology of ordered and non-ordered pore arrays can also be observed at the cleaved edges of the alumina layers. Figure 5 shows the cleaved edge of an ordered and a nonordered sample both produced with 40 V anodizing voltage. The image of the ordered structure was taken at the bottom part of the layer. Only in the case of ordered structures, does cleavage result in flat edges within the ordered domains. The distance of the pore rows in the ordered structure indicates that cleavage proceeded through the pore centers along one axis of the hexagonal lattice. From the pore and cell wall diameters visible in the ordered structure, a porosity of about 10%, as found by Bailey and Wood for anodic alumina layers formed in oxalic acid,¹⁰ can be estimated.

Growth Kinetics

It has been shown in previous studies^{6,7} that low anodization voltages are unfavorable conditions for the

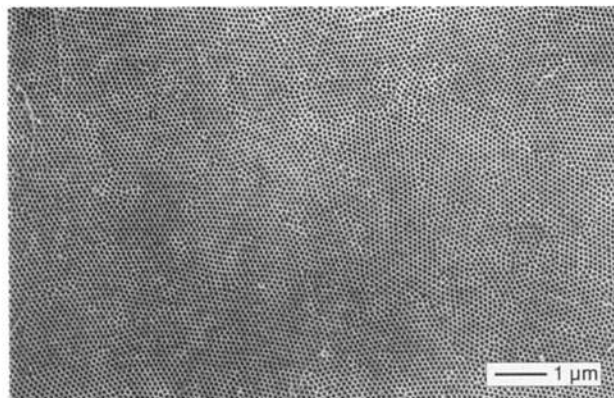


Fig. 3. SEM bottom view of an anodic alumina layer after dissolution of the pore bottoms by chemical etching showing a polycrystalline pore lattice [40 V, 0.3 M (COOH)₂, 1°C].

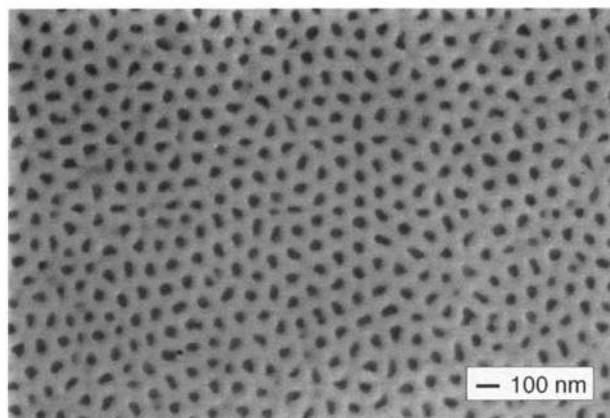


Fig. 4. SEM bottom view of a nonordered pore structure in anodic alumina [40 V, 0.3 M (COOH)₂, 1°C].

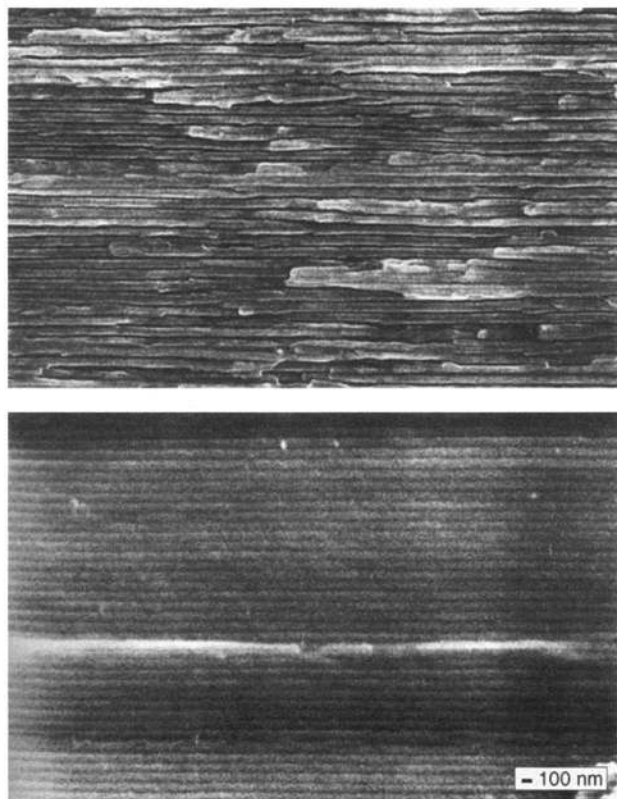


Fig. 5. SEM images of the cleaved edge of a nonordered (upper image) and of the lower part of an ordered alumina layer (lower image).

formation of ordered pore structures. This finding has been attributed to the volume expansion of the aluminum during the oxidation process, which occurs only at high anodization voltages and leads to repulsive forces between neighboring pores.⁶ On the other hand, ordered pore arrays are also not observed at very high voltages, although a strong volume expansion of the aluminum during oxidation takes place under these conditions. In order to provide a possible explanation for this behavior, the voltage dependence of the oxidation kinetics is discussed in the following section.

Formation of porous anodic alumina under potentiostatic conditions starts with the formation of a barrier oxide up to a thickness determined by the applied voltage at which the oxide becomes insulating against ionic conduction. Subsequently, pores nucleate and grow with the bottoms covered by a barrier oxide layer.^{9,11,12} Finally, a regime of steady-state pore growth is reached. It is characterized by balance between field-enhanced oxide dissolution at the oxide/electrolyte interface at the pore bottoms and formation of oxide at the metal/oxide interface due to migration of O^{2-}/OH^- ions through the bottom oxide layer.^{9,13} The formation process is accompanied by a high starting current during formation of the initial barrier oxide, a steep current reduction when the oxide becomes insulating against ion migration followed by a rise due to the formation of pores, and a constant current in the regime of steady-state pore growth.¹⁴ When starting from an electropolished aluminum surface, under the conditions applied here the steady state conditions were reached within about 10 min. The variation of the current during the several days of oxidation time applied for the formation of ordered pore arrays is shown in Fig. 6 for different anodization potentials. Since both the ionic migration and the oxide dissolution at the pore bottoms depend strongly on the applied potential, a strong dependence of the current at the beginning of the steady-state pore growth on the potential is observed. Whereas with 30 V anodizing voltage the current is nearly constant over the whole etching time, at high voltages, particularly at 60 V, a strong decrease of the

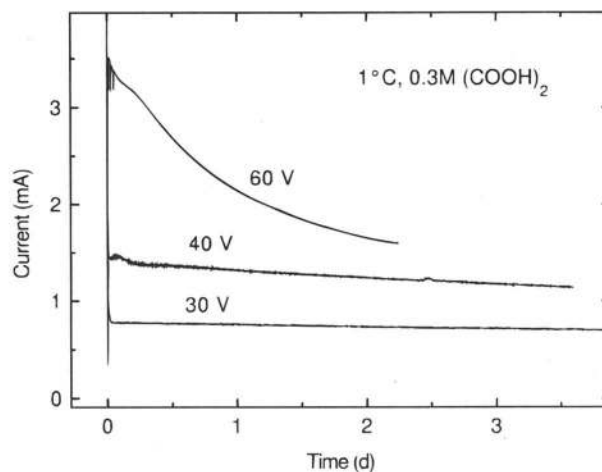


Fig. 6. Oxidation current vs. time for different anodization potentials.

current with time, and therefore with pore depth, is observed. Apparently, for high voltages and currents the etching conditions at the pore bottoms depend strongly on time. The reason for this behavior is the change of the electrolyte composition at the pore bottoms due to chemical reactions associated with the pore growth. Due to incorporation of the anions into the forming alumina, which has been reported for several acids including oxalic acid,¹⁵⁻¹⁸ oxalate ions are consumed during oxidation. Therefore, the concentration of oxalate ions at the pore bottom decreases, leading to a decrease in current. Further changes in the electrolyte composition are due to the consumption of oxygen, which leads to an increase of the H^+ concentration, and the accumulation of hydrated Al^{3+} because of the dissolution of alumina at the pore bottoms. Since the rate of consumption and production of electrolyte species is given by the oxidation rate, high currents lead to a faster change of electrolyte composition at the pore bottoms. Since stirring of the electrolyte does not effect the volume in the pores, the exchange of species between the bulk electrolyte and the pore bottoms is a diffusion-controlled process. Therefore the pore depth also influences the evolution of the current, leading to an even faster decrease of the current at high voltages due to the higher pore growth rate at the beginning of the oxidation.

For the formation of ordered pore arrays, experimental conditions which are favorable for the self-organization process should be maintained over long anodization times. Therefore, experimental parameters which lead to strongly time-dependent etching conditions are not suitable for the formation of ordered structures. Also the high etching rates associated with high voltages should be generally unfavorable for the formation of ordered structures. Despite other changes in the formation conditions for ordered pore arrays with variation of the anodizing voltage,⁶ the lower degree of ordering of the pore structures formed at 60 V compared to that formed at 40 V can be understood from this consideration.

Influence of Experimental Conditions

In the section on sample morphology, it has been shown that ordered pore arrays are related to the existence of a smooth etching front. The latter can likely only be achieved if the anodization is started from a smooth metal surface and specially homogeneous etching conditions are maintained during pore growth. Therefore in the following section, the impact of the pretreatment of the aluminum foils as well as of the anodization conditions on the formation of ordered structures are discussed.

Preannealing of the aluminum substrate.—One necessary condition for the formation of ordered pore arrays was the annealing of the aluminum foils before oxidation in order to enhance the grain size in the metal substrate. It was performed typically for 3 h at 500°C under forming

gas or nitrogen atmosphere. As a result, smooth aluminum foils with grain sizes in the 100 μm range were obtained. Figure 7 shows the surface of an annealed and subsequently electropolished aluminum foil after 3 h of storage in 5 wt % aqueous phosphoric acid at 30°C. The etching behavior is clearly nonhomogeneous. There are straight lines with increased etching rates which are attributed to grain boundaries of the annealed aluminum. Additionally some pinholes are observed with a mean distance in the range of 1 μm . They could be points where dislocations emerge at the surface. The exact nature of this defect is not important, but they clearly show variations in the etching behavior of the starting material. One can conclude that the size of the ordered domains in the hexagonal pore arrays is not determined by the grains in the aluminum metal, which are about 100 times larger than the grains of the pore lattices. On the other hand, the dislocation density in the aluminum is in the range of the density of point defects in the polycrystalline pore lattices (Fig. 3). Nevertheless, there is no direct evidence up to now that defects in the pore lattice can originate from dislocations or other defects in the aluminum. The correlation between the annealing of the aluminum and the formation of ordered pore arrays shows that the process of self-organization is at least disturbed by a large number of grain boundaries in the nonannealed aluminum foils. Since the conditions for oxidation at the grain boundaries are different from those in perfectly crystalline areas, a different pore growth rate, leading to a rough etching front and a nonordered pore lattice, is expected.

Stirring of the electrolyte.—Also the stirring of the electrolyte during oxidation was a necessary condition for obtaining ordered hexagonal structures. Figure 8 shows the reaction of the oxidation current on switching off the stirrer after 2 days of anodization and switching it on again after another two days. The stirring causes a current noise of typically 1–3% of the absolute value. While during stirring the current decreases relatively slowly with time, after switching off the stirrer the current drops below 30% of the former value within 2 days. When the stirrer is switched on again, the current recovers within 10 min to about the level that would be expected after continuous stirring. This behavior can be explained by a model discussed by Patemarakis and Papandreadis.¹⁹ In Fig. 9, the concentration profile for hydrated aluminum ions as a product of the dissolution reactions at the pore bottom is shown along the pore axis with and without stirring of the bulk electrolyte. While the stirrer is operating, the concentration of the dissolution products at the pore mouths is equal to the concentration in the bulk electrolyte, since the electrolyte at and above the alumina surface is continuously exchanged. In the case of aluminum ions this concentration is equal to zero. Since the diffusion rate of aluminum is determined by the concentration gradient, the concentration of aluminum at the pore bottom is a

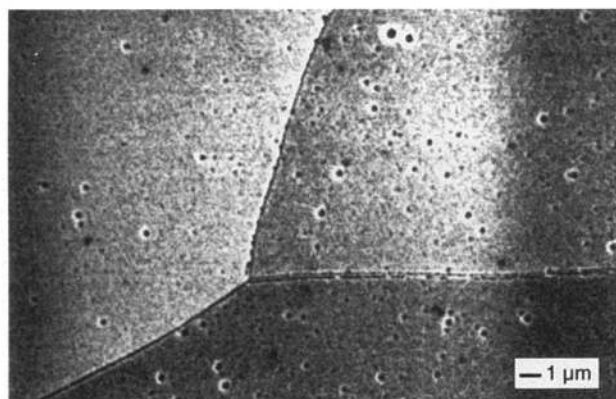


Fig. 7. SEM image of the surface of an aluminum foil after annealing, electropolishing, and 3 h chemical etching in 5 wt % phosphoric acid.

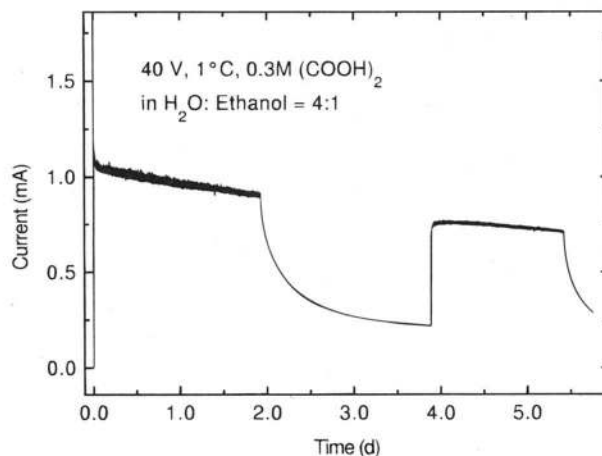


Fig. 8. Current vs time curve when switching the stirrer off and on again.

function of the production rate of aluminum at the pore bottom as well as of the pore depth. When the stirrer is switched off, the aluminum containing electrolyte is no longer removed from the surface. Therefore, an aluminum concentration is also built up in the bulk electrolyte near the alumina surface so that the concentration gradient inside the pores decreases. The results in a lower diffusion rate of aluminum and a higher equilibrium concentration at the pore bottom. The same consideration as for dissolution products is also valid for electrolyte species that are consumed at the pore bottom. For these species, instead of an enhanced accumulation, a higher degree of depletion at the pore bottoms is expected without stirring. A reduction of the concentration of acid anions at the pore bottoms leads to a lower steady-state current compared to anodization with stirring. The rate of change of the concentration profiles after the stirrer is switched off is determined by the diffusion and accumulation in the liquid outside the pores. For this reason, it takes a relatively long time before the new steady-state conditions accompanied by an approximately constant anodization current have been reached. In contrast, the concentrations of the electrolyte components at the surface return immediately to the bulk electrolyte values after switching on the stirrer again. This causes the electrolyte composition at the pore bottoms to return to the steady-state conditions with stirring within a relatively short time. This shorter relaxation time is determined by the diffusion rates of species in the pores and not by the diffusion and accumulation outside the pores, as in the case of switching the stirrer off.

In order to explain the impact of stirring on the formation of ordered pore arrays, two different considerations can be put forward. First, the electrolyte composition at the pore bottoms with and without stirring are largely different, so that the currents differ by more than a factor of three. Therefore, it cannot be expected that ordered structures can be observed both with and without stirring with the other experimental parameters unchanged. From that point of view one may expect that the formation of ordered pore arrays may occur also without stirring, but with other forming volt-

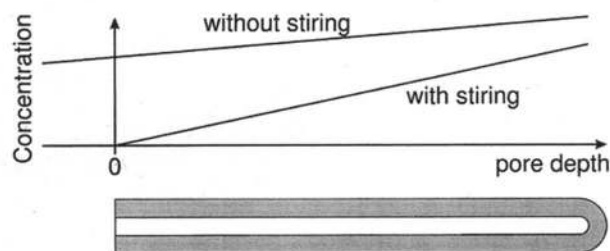


Fig. 9. Concentration profile of aluminum along the pore axis with and without stirring of the bulk electrolyte.

ages or bulk electrolyte concentrations as in the case of a stirred electrolyte. On the other hand, the stirring of the acid may contribute to spatially homogenous etching conditions. Formation of bubbles on the alumina surface can be observed by the eye when the stirrer is not operating. Bubble formation inside the pores is not expected because of the small pore diameters of less than 20 nm. Bubbles can be removed from the surface of the sample by rigorous stirring, so that homogeneous conditions for the transport of electrolyte species are provided over the whole surface. Therefore, we do not expect that the self-organized formation of ordered pore arrays can be obtained without stirring the electrolyte, even when the bulk electrolyte composition is changed in order to compensate for the different concentration profiles along the pore axis.

Influence of surface roughness.—Ordered pore arrays could only be obtained starting from smooth, electropolished aluminum surfaces. After the foils had been electropolished in a 4:4:2 by weight mixture of H_3PO_4 , H_2SO_4 , and H_2O , a surface roughness of typically 20 to 30 nm on a lateral length scale of 10 μm was observed by AFM. As determined by mechanical profiling, the nonpolished surfaces exhibited a roughness of about 5 μm , mainly due to parallel trenches caused by the rolling of the aluminum foils. The oxidation current vs. time with a polished and a nonpolished starting surface is shown in Fig. 10. The lower plot shows the development during the first hours of oxidation time, the upper plot shows the evolution over the whole etching period. In the lower plot, the electropolished sample exhibits a rise of the current associated with the formation of pores after approximately 5 min of etching. In contrast, this rise is observed only after more than 1 h for the nonpolished surface. Also the initial decrease of the current associated with the formation of a continuous barrier oxide proceeds much slower than in the case of the electropolished surface. This means that it takes longer to form a barrier oxide of homogeneous thickness than in the case of a smooth surface.

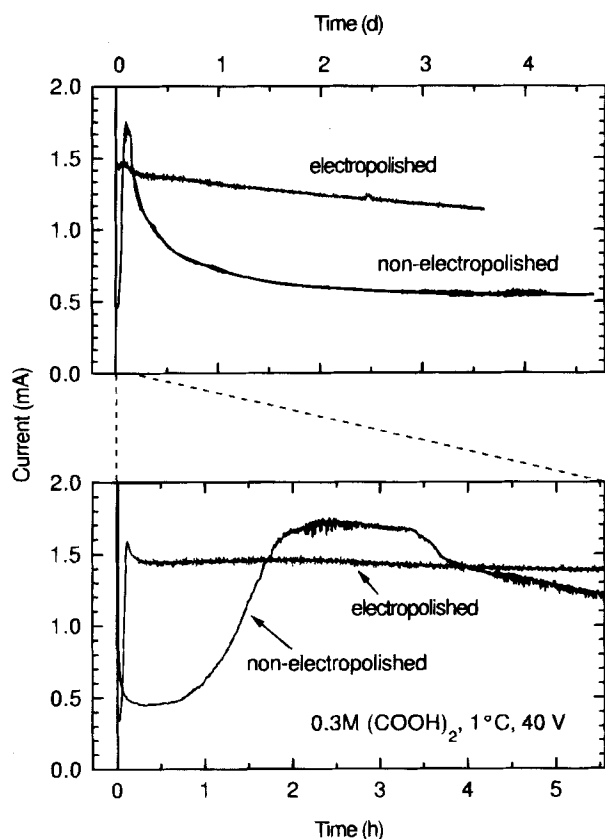


Fig. 10. Current vs. time with and without electropolishing of the starting surface. The upper plot shows the development over the whole etching time, the lower the first hours of oxidation.

The high surface roughness leads to a faster formation of barrier oxide and pores at depressions of the surface than at other locations. The pores that nucleated at such depressions in an early stage will grow in front of the other pores. The surface roughness is thus transferred to the etching front at the interface between the aluminum and oxide layer and prevents self-organization.

Another interesting observation, which can be seen in the upper plot of Fig. 10, is the large current decrease in the early stages of steady-state pore growth for nonelectropolished samples. A natural explanation is the dying out of many of the pores that were left behind, leaving a relatively small number of active pores. A high current concentration in the surviving pores may lead to a current reduction due to strong changes in the electrolyte composition in these pores. In addition, branching of pores, which has been observed in anodic alumina after reduction of the forming voltage,⁸ is a likely effect in the case when only a low number of pores remains active. In this case, the exchange of electrolyte species between the pore bottoms and the surface is severely limited by the low number of active pores that keep the pore bottoms in contact with the electrolyte. This explains the remarkably low current at long anodization times compared to electropolished foils.

As in the case of oxidation in a nonstirred bath, these changes in the electrolyte composition at the pore bottoms can be the reason that no ordered pore arrays are observed with nonelectropolished surfaces. On the other hand, also the correlation between the homogeneous depth of neighboring pores and the formation of ordered structures can account for the low degree of ordering. The observation of entirely flat interfaces between the alumina and the underlying metal in ordered pore arrays indicates that there is some mechanism slowing down the growth rates of the faster growing pores which causes a flattening of the etching front. Such a mechanism can be caused by the self-limiting character of the etching process due to the change in electrolyte composition at the pore bottoms. A higher etching rate in one particular pore will lead to a stronger depletion of acid anions at the pore bottom and to a decrease in the pore growth rate. Most likely such a mechanism does not work in the case of nonelectropolished surfaces in the etching times that were applied in this work. Neither smooth lower surfaces of the alumina nor ordered hexagonal pore structures were observed with nonelectropolished surfaces. Whether this is caused by too short an etching time or whether such a mechanism fails in case of high roughness of the etching front, cannot be decided yet.

Summary

Nearly perfectly ordered hexagonal pore arrays were obtained in anodic alumina with the anodization parameters explored by Masuda and Fukuda.⁵ While the pores nucleated on the upper surface at random positions, a polycrystalline pore structure with a lattice constant of about 100 nm and ordered domains of micron size is observed on the lower surfaces of oxide layers of 100–200 μm thickness. The morphological features were compared to those found in the ordinary nonordered pore structures. Besides differences in the pore shapes and densities, a striking difference in the homogeneity in the depth of neighboring pores and the roughness of the metal/oxide interface was observed. We conclude from this, that the self-organized formation of ordered pore arrays is correlated with a homogeneous depth of neighboring pores.

The existence of entirely flat interfaces in ordered pore structures is an indication for a self-adjusting mechanism which slows down the reaction rate in the fastest growing pores. It is suggested that such a mechanism originates from the self-limiting character of the reactions associated with pore growth at the pore bottoms. The need of a flat etching front explains why spatially inhomogeneous etching conditions prevent the formation of ordered pore arrays. Such inhomogeneities can be caused by material properties like high surface roughness or high density of grain boundaries in the aluminum substrate. Therefore the pretreatment of the start-

ing material in terms of annealing and electropolishing is an important prerequisite for the formation of ordered structures. Also stirring of the electrolyte during anodization, which prevents bubble formation on the surface, is a necessary condition for the process of self-organization.

In order to explain the self-organized formation of ordered structures, a repulsive interaction between neighboring pores during growth has to be assumed. As the origin of such an interaction, mechanical stress due to the expansion during oxidation of the aluminum, which is strongly dependent on parameters like voltage and electrolyte composition, has been proposed.⁶ Since the electrolyte composition at the pore bottoms, and therefore the oxidation current, differs largely from a stirred to a non-stirred bath, different results are obtained under these two experimental conditions. Even in a stirred bath the electrolyte composition at the pore bottoms varies with time, especially at high anodization voltages and pore growth rates. Therefore, moderate voltages, leading to constant conditions over the whole etching time, are favorable for the formation of ordered pore arrays.

Acknowledgments

The authors wish to thank U. Doß and T. Martini for their assistance with the scanning electron and atomic force microscope, respectively.

Manuscript received January 26, 1998.

Max-Planck-Institute für Mikrostrukturphysik assisted in meeting the publication costs of this article.

REFERENCES

1. F. Keller, M. S. Hunter, and D. L. Robinson, *J. Electrochem. Soc.*, **100**, 411 (1953).
2. C. H. Martin, *Chem. Mater.*, **8**, 1739 (1996).
3. H. Masuda and M. Satoh, *Jpn. J. Appl. Phys.*, **35**, L126 (1996).
4. D. Routkevitch, A. A. Tager, J. Harujama, D. Almalawi, M. Moskovits, and J. M. Xu, *IEEE Trans. Electron. Devices*, **ED-40**, 1646 (1996).
5. H. Masuda and K. Fukuda, *Science*, **268**, 1466 (1995).
6. O. Jessensky, F. Müller, and U. Gösele, *Appl. Phys. Lett.*, **72**, 1173 (1998).
7. H. Masuda, F. Hasegawa, and S. Ono, *J. Electrochem. Soc.*, **144**, L127 (1997).
8. H. Masuda, H. Yamada, M. Satoh, A. Atsoh, M. Nakao, and T. Tamamura, *Appl. Phys. Lett.*, **71**, 2770 (1997).
9. J. P. O'Sullivan and G. C. Wood, *Proc. R. Soc. London, Ser. A*, **317**, 511 (1970).
10. G. Bailey and G. C. Wood, *Trans. Inst. Met. Finish.*, **52**, 187 (1974).
11. G. E. Thompson, R. C. Furneaux, G. C. Wood, J. A. Richardson, and J. S. Goode, *Nature*, **272**, 433 (1978).
12. K. Shimizu, K. Kobayashi, G. E. Thompson, and G. C. Wood, *Philos. Mag. A*, **66**, 643 (1992).
13. T. P. Hoar and N. J. Mott, *J. Phys. Chem. Solids*, **9**, 97 (1959).
14. V. P. Parkhutik and V. I. Shershulsky, *J. Phys. D: Appl. Phys.*, **25**, 1253 (1992).
15. Y. Fukuda, *Trans. Natn. Res. Inst. Met.*, **17**, 25 (1975).
16. G. E. Thompson and G. C. Wood, *Nature*, **290**, 230 (1981).
17. G. E. Thompson and G. C. Wood, in *Corrosion: Aqueous Processes and Passive Films*, J. C. Scully, Editor, Academic Press, London (1983).
18. A. Despic and V. P. Parkhutik, in *Modern Aspects of Electrochemistry*, J. O. Bockris, B. E. Conway, and R. E. White, Editors, Plenum Press, New York (1989).
19. G. Paternaraki and N. Papandreadis, *Electrochim. Acta*, **38**, 2351 (1993).

Determination of the Diffusion Coefficient and Phase-Transfer Rate Parameter in LaNi_5 and $\text{MmNi}_{3.6}\text{Co}_{0.8}\text{Mn}_{0.4}\text{Al}_{0.3}$ Using Microelectrodes

Anton Lundqvist and Göran Lindbergh

Department of Chemical Engineering and Technology, Applied Electrochemistry, Royal Institute of Technology, KTH, SE-100 44 Stockholm, Sweden

ABSTRACT

A potential-step method for determining the diffusion coefficient and phase-transfer parameter in metal hydrides by using microelectrodes was investigated. It was shown that a large potential step is not enough to ensure a completely diffusion-limited mass transfer if a surface-phase transfer reaction takes place at a finite rate. It was shown, using a kinetic expression for the surface phase-transfer reaction, that the slope of the logarithm of the current vs. time curve will be constant both in the case of the mass-transfer limited by diffusion or by diffusion and a surface-phase transfer. The diffusion coefficient and phase-transfer rate parameter were accurately determined for $\text{MmNi}_{3.6}\text{Co}_{0.8}\text{Mn}_{0.4}\text{Al}_{0.3}$ using a fit to the whole transient. The diffusion coefficient was found to be $(1.3 \pm 0.3) \times 10^{-13} \text{ m}^2/\text{s}$. The fit was good and showed that a pure diffusion model was not enough to explain the observed transient. The diffusion coefficient and phase-transfer rate parameter were also estimated for pure LaNi_5 . A fit of the whole curve showed that neither a pure diffusion model nor a model including phase transfer could explain the whole transient.

Introduction

The increased use of LaNi_5 alloys as the negative electrode in secondary batteries has initiated a lot of research to determine their physiochemical parameters. Such parameters are the rate constants and diffusion coefficients. Diffusion has been studied using both electrochemical and other methods. Results of different methods, also nonelectrochemical, have been compiled by Zheng et al.¹ They determined the diffusion coefficient in $\text{LaNi}_{4.25}\text{Al}_{0.75}$, using constant-potential and constant-current discharge techniques, to be $3 \times 10^{-15} \text{ m}^2/\text{s}$. They also studied bare and copper-coated $\text{LaNi}_{4.27}\text{Sn}_{0.24}$ using a constant-current

method, measuring a diffusion coefficient of $6.75 \times 10^{-15} \text{ m}^2/\text{s}$.² Valøen et al. used electrochemical impedance spectroscopy to determine a diffusion coefficient in the range of 10^{-13} to $10^{-14} \text{ m}^2/\text{s}$, depending on the state of charge for $\text{MmNi}_{3.5-3.7}\text{Co}_{0.7-0.8}\text{Mn}_{0.3-0.4}\text{Al}_{0.3-0.4}$.³ A potential-step method was used by Iwakura et al. to determine the diffusion coefficient for $\text{MmNi}_{4.3}\text{Al}_{0.5}\text{Mn}_{0.3}$ in the range 0.5 to $3 \times 10^{-12} \text{ m}^2/\text{s}$, where M represents Co, Cr, Fe, Mn, or Ni.⁴

There have been only a few studies of the diffusion coefficient of pure LaNi_5 using electrochemical methods, due to the corrosion sensitivity and brittleness of the material. However, Züchner et al. studied diffusion in the α -phase of a single-crystal membrane and determined the diffusion